On Validity of Constant pH Simulations

Amin Bakhshandeh and Yan Levin*

Instituto de Física, Universidade Federal do Rio Grande do Sul, Caixa Postal 15051, CEP 91501-970, Porto Alegre, RS, Brazil.

E-mail: levin@if.ufrgs.br

Abstract

Constant pH (cpH) simulations are now a standard tool for investigating charge regulation in coarse-grained models of polyelectrolytes and colloidal systems. Originally developed for studying solutions with implicit ions, extending this method to systems with explicit ions or solvent presents several challenges. Ensuring proper charge neutrality within the simulation cell requires performing titration moves in sync with the insertion or deletion of ions – a crucial aspect often overlooked in the literature. Contrary to prevailing views, cpH simulations are inherently grand-canonical, meaning that the controlled pH is that of the reservoir. The presence of the Donnan potential between the implicit reservoir and the simulation cell introduces significant differences between titration curves calculated for open and closed systems – the pH of an isolated (closed) system is different from the pH of the reservoir, for the same protonation state of the polyelectrolyte. To underscore this point, in this paper we will compare the titration curves calculated using the usual cpH algorithm with those from the exact canonical simulation algorithm. In the latter case, titration moves adhere to the correct detailed balance condition, and pH is calculated using the recently introduced surface Widom insertion algorithm. Our findings reveal a very significant difference between the titration isotherms obtained using the standard cpH algorithm and the canonical titration algorithm, emphasizing the importance of using the correct simulation

https://doi.org/10.26434/chemrxiv-2024-6tqm6 **ORCID:** https://orcid.org/0000-0001-5448-5179 Content not peer-reviewed by ChemRxiv. **License:** CC BY 4.0

approach when studying charge regulation of polyelectrolyte, proteins, and colloidal particles.

Introduction

The effective charge of colloidal particles and polymers, produced by weak acid or weak base functional groups, experiences variation with environmental pH due to the ionization of these groups.[1–15] The $\mathrm{pH} = -\log_{10}(a_{\mathrm{H}})$,[16] is defined as the negative decadic logarithm of dimensionless proton activity, $a_{\mathrm{H}} = c_{\mathrm{H}} \mathrm{e}^{\beta \mu_{\mathrm{H}}^{ex}} / c^{\ominus}$, where $c^{\ominus} = 1$ M is the standard concentration, $\beta = 1/k_B T$, and μ_H^{ex} denotes the excess electrochemical potential.[17]

The stability of colloidal particles in aqueous suspensions is intrinsically connected with their surface charge density, which is controlled by the pH of solution. Similarly, the activity of many biologically relevant proteins and polyelectrolytes is influenced by the solution's pH and ionic strength.[6,13,17–34] Quantitative understanding of charge regulation in such complex systems is, therefore, crucial for a wide range of industrial and medical applications.

For some simple colloidal systems, one can use the Poisson Boltzmann theory with the charge regulation boundary condition to study the degree of protonation.[1,2,10–12,14,15,35–41] However, this approach breaks down for suspensions containing salts with multivalent counterions or when studying flexible molecules – such as proteins, polyelectrolytes, polyampholytes etc., whose three-dimensional conformation is directly determined by the protonation state of the macromolecules. To overcome this difficulty, in 1992 Reed & Reed (RR) proposed a constant pH (cpH) Monte-Carlo simulation method,[3,42] to calculate the titration curves for such systems. Originally the RR-cpH algorithm was applied to systems with implicit ions – the monomers interact with each other through the screened Coulomb potential – soon after, however, extensions to systems with explicit ions were proposed.[3] To preserve the overall charge neutrality in such approaches, a protonation move is combined with an arbitrary deletion of one hydronium ion inside the cell and a deprotonation move with an

https://doi.org/10.26434/chemrxiv-2024-6tqm6 **ORCID:** https://orcid.org/0000-0001-5448-5179 Content not peer-reviewed by ChemRxiv. **License:** CC BY 4.0

arbitrary insertion of a hydronium ion at a random position inside the cell. Such arbitrary insertion/deletion of ions inside the simulation cell, however, violates the detailed balance condition, leading to incorrect results.[43–45] The problem with the RR-cpH algorithm, when applied to explicit ions, was pointed out some 20 years ago by Labbez & Jönsson,[43] but unfortunately went unnoticed inside the physical chemistry and soft matter communities, where RR-cpH became very popular to treat various systems in which charge regulation plays important role.[3] An alternative canonical approach to calculate the titration curves was proposed by Ullner and Woodward. These authors used a closed spherical simulation cell with a fixed number of protons. They then used Widom insertion method to obtain the chemical potential inside the system for a given protonation state.[46]

Contrary to a common misconception, RR-cpH algorithm is not a canonical algorithm.[47] For isolated systems the total number of protons is conserved and the titration algorithm must use the correct *canonical* acceptance probabilities for the protonation/deprotonation moves, which do not explicitly depend on the pH inside the simulation cell.[44,48–50] In a canonical (isolated) system, pH is not a control parameter – it can not be specified *a priori*, but only be calculated *a posteriori*, after the simulation has fully equilibrated and the number of protonated groups has been determined.[50] Therefore, if one wants to modify the RR-cpH algorithm to properly include the explicit ions, one must take into account that the simulation cell is implicitly in contact with an external reservoir of acid and salt.[44,51] A protonation/deprotonation move should then be combined with a simultaneous insertion/deletion of an anion from the reservoir, in accordance with the correct *grand canonical* acceptance probability.[43,44,51] Furthermore, since in such simulation polyelectrolyte is confined within the cell, while ions can freely exchange between the system and the reservoir, the two will be at different electrostatic potentials.[45,51] This is known as the "Donnan potential", φ_D. Presence of the Donnan potential between the implicit reservoir and the simulation cell introduces significant difference between titration curves calculated for open and closed systems – the pH_c of an isolated (closed) system is different from the pH_R of the reservoir,

https://doi.org/10.26434/chemrxiv-2024-6tqm6 **ORCID:** https://orcid.org/0000-0001-5448-5179 Content not peer-reviewed by ChemRxiv. **License:** CC BY 4.0

for the same protonation state of the polyelectrolyte.[44,45,52] When discussing pH of inhomogeneous systems, such as a polyelectrolyte solution separated from the reservoir of acid and salt by a semipermeable membrane, it is usual to define activity by separating the mean-electrostatic potential within the phase. Such definition is equivalent to placing the reference (saturated calomel) and hydrogen electrodes within the same phase when measuring the pH.[52] The equivalence of electrochemical potential of hydronium ions across the membrane is then expressed as $\ln a_H^S + \beta q\, \varphi_D = \ln a_H^R$, where a_H^S is the activity of hydronium ions inside the polyelectrolyte solution (system) and a_H^R is the activity inside the reservoir. The pH inside the system is then defined as $\mathrm{pH}_S = -\log_{10}(a_{\mathrm{H}}^S)$ and inside the reservoir as $\mathrm{pH}_R = -\log_{10}(a_{\mathrm{H}}^R)$. In a recent paper we have discussed the problems that may arise due to the violation of the Gibbs-Guggenheim principle,[52] when mean-electrostatic potential is excluded from the definition of activity. Nevertheless, since this is the usual convention, we will adopt it in the present paper. The pH inside the system is then different from that of the reservoir[46]. Furthermore, if after the equilibrium is established, the system is disconnected from the reservoir (is closed) its pH_S will not be affected. Therefore, if we would perform a canonical reactive simulation on such a closed system, we will obtain exactly the same pH, i.e. $\mathrm{pH}_c = \mathrm{pH}_S$. The relation between pH inside the system and pH in the reservoir is then:[45]

$$\mathrm{pH}_S = \mathrm{pH}_R + \frac{q\beta\varphi_D}{\ln(10)} \tag{1}$$

This allows us to use grand canonical simulations, in which the chemical potential of hydronium ions (pH_R) is specified inside the reservoir, to determine the pH_c=pH_S inside an isolated system. To do this, however, requires the knowledge of the Donnan potential difference between the system and the reservoir.

To preserve the charge neutrality, usual grand canonical simulation methods involve insertions of neutral pairs of ions into the system – making the Donnan potential cancel in the acceptance probability of such pair moves. This prevents us from obtaining the Donnan potential using such approaches.[51,53] Therefore, a corrected constant pH algorithm – in which

https://doi.org/10.26434/chemrxiv-2024-6tqm6 **ORCID:** https://orcid.org/0000-0001-5448-5179 Content not peer-reviewed by ChemRxiv. **License:** CC BY 4.0

the charge neutrality is properly taken into account through the pairwise insertions – will only allow us to calculate the protonation state of polyelectrolyte as a function of pH_R inside the reservoir and not the pH_S inside the system (simulation cell). On the other hand, most experiments are conducted on closed systems, which according to Eq. (1) will have different pH from that of the reservoir. Recently we have developed a new reactive grand canonical Monte Carlo Donnan (rGCMCD) simulation method that allows us to calculate both the Donnan potential and the protonation state of polyelectrolyte solution in contact with a reservoir of acid and salt.[45] Eqn. (1) then permits us to simultaneously calculate the titration isotherms for an open system, as a function of pH in the reservoir; and for a closed system, as a function of pH inside the simulation cell.

If one is interested in studying closed systems, rGCMCD approach is not very convenient since it calls for the specification of the chemical potential of all ions inside the reservoir in order to perform the grand canonical moves. This requires a separate simulation of the reservoir in which Widom insertion method is used to obtain the chemical potential of all the ions.[54–58] Furthermore, the calculation of the Donnan potential within the grand canonical formalism makes such simulations slow. Recently we have developed a new method for canonical titration simulations utilizing the surface Widom insertion algorithm that enables us to easily calculate equilibrium pH.[50] In such systems, the traditional Widom insertion method can not be used, since at high pH there maybe few or no hydronium ions present inside the simulation cell, preventing us from accurately determining the chemical potential of these ions. The difficulty of calculating pH in canonical reactive simulations is probably one of the reasons for the widespread use of the incorrect RR-cpH algorithm in the soft mater and biophysics literature.[3]

The primary objective of this paper is to quantitatively explore the limitations of the RR-cpH algorithm. To achieve this, we compare the RR-cpH algorithm with three different methods: the surface Widom canonical reactive simulation, the rGCMCD simulations, and the pair insertion simulations for systems with high salt content. At high ionic strength, the

https://doi.org/10.26434/chemrxiv-2024-6tqm6 **ORCID:** https://orcid.org/0000-0001-5448-5179 Content not peer-reviewed by ChemRxiv. **License:** CC BY 4.0

Donnan potential vanishes, and the titration isotherms for open and closed systems become identical. We will see that canonical, pair, and rGCMCD methods agree perfectly between themselves, while they disagree strongly from the RR-cpH algorithm – showing its complete failure under a very wide range of experimental conditions.

RR-cpH algorithm

In this methodology, dissociation and association reactions of polyelectrolyte monomers occur with probabilities linked to the acid dissociation constant K_a of the reaction[3]

$$\mathrm{HA} \leftrightarrow \mathrm{H}^+ + \mathrm{A}^-. \tag{2}$$

For the forward direction (deprotonation), a site of a polyelectrolyte undergoes change from 0 to $-q$, where q is the proton charge, while simultaneously, a hydronium ion is "created" at a random position inside the cell. Conversely, in the backward reaction (protonation move), a negatively charged site is neutralized and simultaneously, one random hydronium ion is deleted from the cell. The simulation starts with a charge neutral system, so that for each negative site of polyelectrolyte, there is a hydronium ion present in the bulk of the cell.

The acceptance probabilities for forward and reverse reactions are::[3,44]

$$\mathrm{P} = \min\left[1, \exp\left(-\beta\Delta U + \zeta\left(\mathrm{pH} - \mathrm{pK}_a\right)\ln(10)\right)\right], \tag{3}$$

where ΔU is the change in electrostatic energy, $\mathrm{pK}_a = -\log_{10}(K_a/c^{\ominus})$, and $\zeta = \pm 1$ for deprotonation and protonation moves, respectively.

In the RR-cpH algorithm, one specifies the pH and concentrations of ions and polyelectrolyte inside the simulation cell as the input parameters. The method then provides the degree of ionization, along with ensemble averages of observables after equilibrium has been established. It is often stated that pH in Eq. 3 corresponds to the pH inside the canonical

https://doi.org/10.26434/chemrxiv-2024-6tqm6 **ORCID:** https://orcid.org/0000-0001-5448-5179 Content not peer-reviewed by ChemRxiv. **License:** CC BY 4.0

simulation cell.[47] This, however, is not correct. In a canonical reactive Monte Carlo simulation, the total number of protons inside the system is fixed, simulation algorithm then determines how many of these protons will remain free (in the form of hydronium ions) and how many will become associated with the polyelectrolyte surface groups. The pH of the system, which is related to the electrochemical potential of hydronium ions, does not make part of the detailed balance condition and can not appear in the acceptance probabilities of titration moves. The correct canonical reactive Monte Carlo algorithm will be presented in the following section.

In order to understand the shortfalls of Eq. 3, it's crucial to first recognize that RR-cpH algorithm is inherently grand-canonical. This is evident when examining the weight for a protonation move in Eq. 3, in which appears $e^{-\ln(10)\mathrm{pH}} \sim e^{\beta\mu_H}$, where μ_H is the electrochemical potential of a hydronium ion. This is precisely the grand canonical weight associated with transferring a hydronium ion from the reservoir into the simulation cell. In the context of the Grand Canonical Monte Carlo (GCMC) simulations of Coulomb systems, maintaining charge neutrality within the simulation cell is paramount, in particular when using Ewald summation to treat long-range Coulomb interaction. Consequently, a grand canonical protonation move necessitates a corresponding grand-canonical insertion move for an anion, and a deprotonation move should be coupled with a GCMC removal of an anion, to preserve the overall charge neutrality inside the system. One can't arbitrarily delete or create ions inside the simulation cell, as is usually done in the framework of RR-cpH algorithm.[3] Instead, ions must be inserted or removed from the system with the correct grand-canonical acceptance probabilities.

Canonical ensemble method

Consider now a closed system containing polyions with titratable surface groups, salt, and acid. We can start the system in a initial state in which all polyelectrolyte groups are com-

https://doi.org/10.26434/chemrxiv-2024-6tqm6 **ORCID:** https://orcid.org/0000-0001-5448-5179 Content not peer-reviewed by ChemRxiv. **License:** CC BY 4.0

pletely deprotonated, with the corresponding number of hydronium ions placed in the bulk of the simulation cell. The cell also contain ions derived from the dissociation of salt, say Na^+ and Cl^-. The reactive MC simulation then determines how many of polyelectrolyte groups will become protonated in equilibrium. The acceptance probabilities for deprotonation/protonation moves are given by[44,48–50]

$$\begin{aligned} \mathrm{P}_d &= \min\left[1, \frac{VN_AK_a}{N_\mathrm{H}+1} e^{-\beta\Delta U}\right] \\ \mathrm{P}_p &= \min\left[1, \frac{N_\mathrm{H}}{VN_AK_a} e^{-\beta\Delta U}\right] \end{aligned} \tag{4}$$

where, N_H is the number of free hydronium ions inside the simulation cell at a given moment and N_A is the Avogadro number. Note that for canonical (closed) systems, the acceptance probabilities do not explicitly depend on pH. The pH of the system, after the equilibrium is established, has to be calculated using a separate procedure that require determination of the chemical potential of hydronium ions inside the simulation cell. The conventional approach of employing Widom's particle insertion method encounters practical challenges for moderate and high pH, when cell's interior has few or maybe even no free hydroniums at all, resulting in a very inaccurate reading of the chemical potential of hydronium ions. To overcome this difficulty, we have recently introduced a surface Widom insertion algorithm, which allows us to easily calculate the pH inside the system after equilibrium has been established.[50]

One difficulty when working with Coulomb systems is that we can not cutoff the long range electrostatic interactions between particles and use simple periodic boundary conditions. Instead the system has to be infinitely replicated. To efficiently sum the replicas, we use Ewald summation method, which effectively creates a spherical macroscopic crystal comprised of periodically replicated microscopic simulation cells.[59–62] Typically a simulation cell will have a net electric dipole moment $\boldsymbol{M} = \sum_i q_i \boldsymbol{r}_i$, and a finite second moment tensor of the charge density. Electrostatically, the field produced by a dielectric sphere of uniform polarizability $\boldsymbol{M}$ is equivalent to that of a sphere with non-uniform surface charge density

https://doi.org/10.26434/chemrxiv-2024-6tqm6 **ORCID:** https://orcid.org/0000-0001-5448-5179 Content not peer-reviewed by ChemRxiv. **License:** CC BY 4.0

$\boldsymbol{M} \cdot \boldsymbol{n}/V$, where $\boldsymbol{n}$ represents the unit normal to the surface of the macroscopic sphere. The existence of an effective surface charge induces an electric field within the crystal's interior. Simultaneously, existence of a non-zero second moment tensor of the charge density in the simulation cell results in a dipole layer at the macroscopic crystal's surface.[45,63] This leads to a difference between the mean electrostatic potential inside and outside the crystal. This potential difference is known as the Bethe potential:[50]

$$\phi_B = -\frac{2\pi}{3\epsilon_w V} \sum_i q_i {\boldsymbol{r}_i}^2, \tag{5}$$

where ϵ_w is the dielectric constant of the medium (water). To quantitatively explore the difference between the titration isotherms calculated using the standard RR-cpH algorithm, Eq. 3, and the canonical algorithm Eq. 4, we focus on a colloidal particle with Z active surface groups, placed at the center of a cubic simulation cell of volume $V = L^3$, where L is the side length of the cell. The cell also contain H_3O^+, Cl^-, and Na^+ ions, ensuring the overall charge neutrality. We execute the reactive Monte Carlo simulation to ascertain the average number of protonated surface groups after equilibrium has been established. We then use the surface Widom insertion method to obtain the pH inside the system.[50] Briefly the idea behind the surface Widom method involves bringing a virtual proton from infinity to a randomly chosen colloidal active site. If the selected site is unoccupied (bearing charge $-q$), it "reacts" with the virtual proton, causing its charge to transition to 0. We then calculate the change in the electrostatic energy between the initial and final states ΔU. If the site is already occupied, ΔU is infinite. The system's pH is then given by,[50]

$$\begin{aligned} \mathrm{pH} = &- \log_{10}\left(\frac{N+1}{Z}\right) + \mathrm{pK}_a + \\ &\log_{10}\left(\left\langle \mathrm{e}^{-\beta(\Delta U + q\phi_B)} \right\rangle_0\right), \end{aligned} \tag{6}$$

where N is the number of protonated sites at equilibrium. The average in Eqn. (6) is calculated using 5,000 uncorrelated virtual proton insertions, and the subscript 0 on the

https://doi.org/10.26434/chemrxiv-2024-6tqm6 **ORCID:** https://orcid.org/0000-0001-5448-5179 Content not peer-reviewed by ChemRxiv. **License:** CC BY 4.0

brackets signifies that the evolution of the system between the virtual proton insertion events is performed with the unperturbed Hamiltonian.

The electrostatic energy inside the system is calculated using the Ewald formalism:[45]

$$
\begin{aligned}
U = & \frac{1}{2} \sum_{ij}{}' \sum_{\boldsymbol{n}} \frac{q_i q_j \mathrm{erfc}(\kappa_e |\boldsymbol{r}_i - \boldsymbol{r}_j - L\boldsymbol{n}|)}{\epsilon_w |\boldsymbol{r}_i - \boldsymbol{r}_j - L\boldsymbol{n}|} \\
& + \sum_{k \neq 0} \frac{2\pi \exp(-\boldsymbol{k}^2/4\kappa_e)}{\epsilon_w V \boldsymbol{k}^2} (A(\boldsymbol{k})^2 + B(\boldsymbol{k})^2) \\
& - \sum_i \frac{q_i^2 \kappa_e}{\epsilon_w \sqrt{\pi}} - \frac{Q_t^2}{2\epsilon_w V \kappa_e^2} + \frac{2\pi}{3\epsilon_w V} \boldsymbol{M}^2,
\end{aligned} \tag{7}
$$

where

$$
\begin{aligned}
A(\boldsymbol{k}) &= \sum_i q_i \cos(\boldsymbol{k} \cdot \boldsymbol{r}_i), \\
B(\boldsymbol{k}) &= \sum_i q_i \sin(\boldsymbol{k} \cdot \boldsymbol{r}_i).
\end{aligned} \tag{8}
$$

In Eq. (7), $\boldsymbol{n} = (n_1, n_2, n_3)$ are the integer vectors, $\boldsymbol{k} = (\frac{2\pi}{L} n_1, \frac{2\pi}{L} n_2, \frac{2\pi}{L} n_3)$ are the reciprocal lattice vectors, $Q_t = \sum_i q_i$ is the total charge inside the simulation cell, and κ_e is the damping parameter. The prime on the first sum of Eq. (7) signifies the exclusion of the terms $i = j$ for $\mathbf{n} = 0$. In the calculation of U we use the tin foil boundary condition[50] that eliminates the $\boldsymbol{M}^2$ term in Eq. (7). Note that if one places a virtual proton into the system, it will no longer be charge neutral. A periodically replicated charge non-neutral system will have infinite energy. To avoid this in the calculation of Eq. (7), we have introduced a uniform neutralizing background.[45] In practice, to calculate Ewald sums we used 600 k-vectors. The damping parameter is set to $\kappa_e = 5/L$, so that we can use simple periodic boundary conditions for calculating the short range – erfc term in Eq. (7) – contribution to the total electrostatic energy.

Titration is performed by adding NaOH base to the system. Since hydrolysis of water

https://doi.org/10.26434/chemrxiv-2024-6tqm6 **ORCID:** https://orcid.org/0000-0001-5448-5179 Content not peer-reviewed by ChemRxiv. **License:** CC BY 4.0

is so weak, addition of one OH^- will result in a reaction with hydronium ion inside the cell and appearance of a new water molecule. Within the present implicit water model, addition of one sodium hydroxide molecule is then equivalent to replacing one proton inside the simulation cell with a sodium ion, $H^+ \longrightarrow Na^+$. Therefore, to vary pH, we simply replace one of the protons by Na^+ and rerun the simulation. This will result in a new polyelectrolyte charge and new equilibrium pH. Repeating this procedure until all protons inside the cell have been replaced by sodium ions, we obtain the full titration curve.

Semi-grand canonical reactive Monte Carlo

We next briefly discuss how the RR-cpH algorithm can be modified to properly account for the requirement of charge neutrality inside the simulation cell. As was stressed previous, RR-cpH algorithm is intrinsically grand canonical. Therefore, we must treat the system as if it is connected to a reservoir of acid and salt. In a physical system this would require presence of a semipermeable membrane, which would allow for a free exchange of ions, but would restrict the motion of polymers to the system's interior. Since the concentration of counterions is larger inside the system than in the reservoir, they will tend to diffuse into reservoir, resulting in electric field and a potential drop across the membrane. This is the physical origin of the Donnan potential, φ_D.

The reactive grand canonical Donnan Monte Carlo (rGCMCD), involves the usual grand canonical insertion and deletion moves of individual ions. To preserve the overall charge neutrality inside the cell, a neutralizing background, must also be taken into account. The acceptance probabilities for protonation and deprotonation moves are given by:[45]

$$\begin{aligned} \phi_p &= 10^{\mathrm{pK}_a - \mathrm{pH}} \mathrm{e}^{-\beta(\Delta U_{ele} + q[\varphi_D + \phi_B])}, \\ \phi_d &= 10^{\mathrm{pH} - \mathrm{pK}_a} \mathrm{e}^{-\beta(\Delta U_{ele} - q[\varphi_D + \phi_B])}. \end{aligned} \tag{9}$$

https://doi.org/10.26434/chemrxiv-2024-6tqm6 **ORCID:** https://orcid.org/0000-0001-5448-5179 Content not peer-reviewed by ChemRxiv. **License:** CC BY 4.0

Throughout the simulation, the Donnan potential φ_D is automatically adjusted to drive the system to a charge neutral state.[45] The pH in the above equation refers to that of the reservoir, however, knowledge of φ_D, also allows us to simultaneously calculate the pH_c inside an isolated canonical system using Eq.(1).[45] We should also note that the presence of a neutralizing background requires a modification of the Bethe potential, ϕ_B.[45] We stress again that pH of the reservoir is not the same as of an isolated system of the same ionic content.

We can also combine a protonation move with a grand canonical insertion of an anion into a simulation cell and a deprotonation move with a grand canonical removal of an anion from the cell. The probabilities of such pair moves are respectively:

$$\begin{aligned} \mathrm{P}_p &= \min\left[1, \frac{c^{\ominus} V N_A 10^{\mathrm{pK}_a - \mathrm{pH} - \mathrm{pCl}}}{(N_{\mathrm{Cl}}+1)} e^{-\beta\Delta U}\right] \\ \mathrm{P}_d &= \min\left[1, \frac{N_{\mathrm{Cl}} 10^{\mathrm{pH} - \mathrm{pK}_a + \mathrm{pCl}}}{c^{\ominus} V N_A} e^{-\beta\Delta U}\right], \end{aligned} \tag{10}$$

where $\mathrm{pCl} = -\log_{10}(a_{\mathrm{Cl}})$. Note that the Donnan and Bethe potentials cancel out in the pair moves. This algorithm allows us to calculate the protonation state of polyions as a function of pH and salt concentration *inside the reservoir*. For systems of large volume fractions and low ionic strength such titration curves will differ significantly from the titration curves of isolated systems of the same polyelectrolyte concentration and salt content.[45] However, if the reservoir contains large concentration of salt, the Donnan potential will be very small and the difference between pH of canonical and grand-canonical systems will vanish, see Eq. (1). This provides us with an additional check of consistency of different simulation methods presented here. For large ionic strengths, the canonical, rGCMCD, Eq. (9), and the pair insertion algorithms, Eq. (10), should both produce identical titration curves.

https://doi.org/10.26434/chemrxiv-2024-6tqm6 **ORCID:** https://orcid.org/0000-0001-5448-5179 Content not peer-reviewed by ChemRxiv. **License:** CC BY 4.0

Results

To compare the predictions of the RR-cpH algorithm with the canonical titration method, we consider a colloidal particle of radius of 60 Å and $Z = 600$ surface groups. Simulations are carried out within a cubic box of side lengths L, containing a colloidal particle at its center. Ewald summation is used to account for Coulomb interactions. In the spirit of coarse grained RR-cpH algorithm, we use the primitive model of solvent that treats water as a uniform dielectric continuum of Bjerrum length $\lambda_B = q^2/(k_B T \epsilon_w) = 7.2$ Å. Active functional groups have intrinsic $pK_a = 5.4$. The simulation cell also contains ions H_3O^+, Cl^-, and Na^+, which we all treat as hard spheres of radius 2 Å with a point charge located at the center.

In Fig. 1 we present the titration isotherm of colloidal particles in suspension of volume fraction 11%, containing 10 mM NaCl.

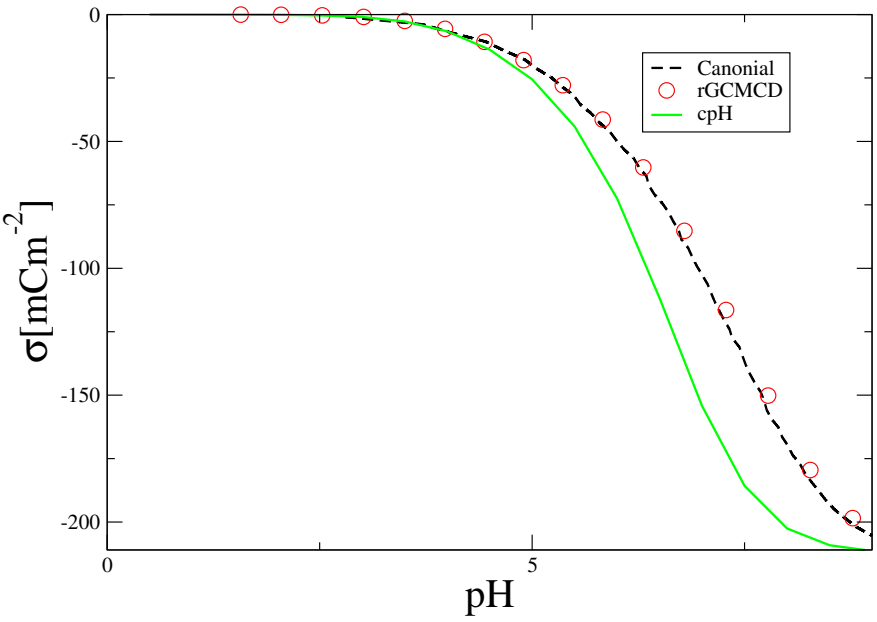

Figure 1: Titration curve for colloidal suspension of 11% volume fraction in the presence of 10 mM salt inside the system. The solid line represents RR-cpH algorithm, the dashed line represents the canonical simulations, and circles are the results obtained using rGCMCD algorithm and Eq. 1 to relate the pH of the reservoir to the pH inside the system.

Fig. 1 clearly shows that there is a very significant disparity between the results obtained

https://doi.org/10.26434/chemrxiv-2024-6tqm6 **ORCID:** https://orcid.org/0000-0001-5448-5179 Content not peer-reviewed by ChemRxiv. **License:** CC BY 4.0

using RR-cpH algorithm and the canonical-Widom reactive simulation algorithm. Furthermore, the figure also shows that the canonical simulation is in perfect agreement with the results obtained using rGCMCD method (indicated by the circles), demonstrating the consistence between two very different approaches. We must conclude that for such systems, the usual implementation of the RR-cpH algorithm is simply wrong.

For systems containing large salt concentration, 100 mM, the disparity between cpH algorithm and canonical simulations diminishes, but still remain very significant for intermediate and large pH, as is illustrated in Fig. 2.

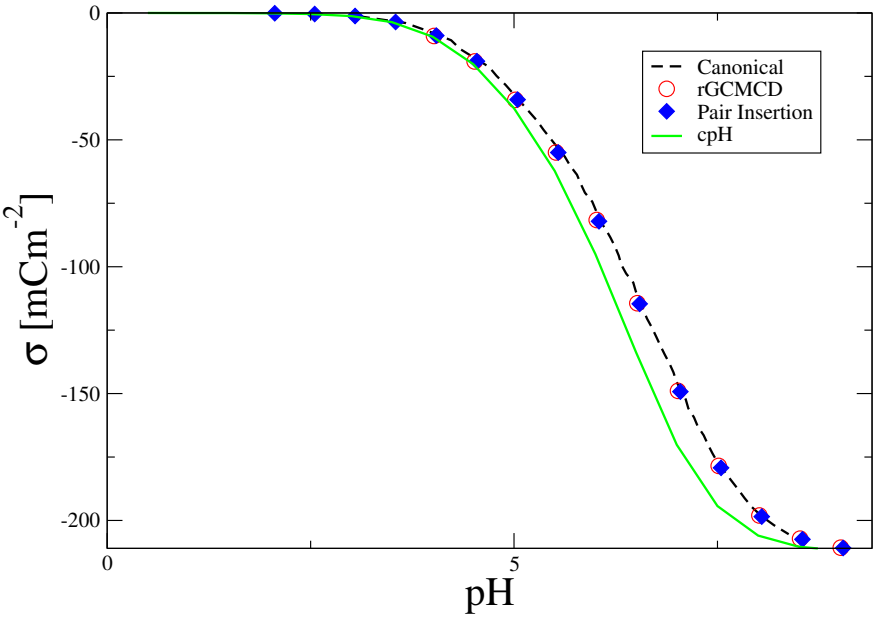

Figure 2: Titration curve for colloidal suspension of 11% volume fraction in the presence of 100mM salt inside the system. The solid line represents RR-cpH algorithm, the dashed line represents the canonical simulation, the circles are the results obtained using rGCMCD and Eq. 1 to relate the pH of the reservoir to the pH inside the system. The solid (blue) squares are the result of pair-insertion algorithm, Eq. (10). Note that for large ionic strengths, Donnan potential vanishes, and canonical and grand canonical titration curves become identical.

On the other hand, we see a perfect agreement between the canonical, rGCMCD Eq.(9), and the pair insertion simulations, Eq. (10). Recall that for large ionic strengths, the Donnan potential vanishes and the pH of the reservoir is the same as inside the system. Under such conditions, there is no difference between canonical and grand canonical titration curves.

https://doi.org/10.26434/chemrxiv-2024-6tqm6 **ORCID:** https://orcid.org/0000-0001-5448-5179 Content not peer-reviewed by ChemRxiv. **License:** CC BY 4.0

Finally, we compare RR-cpH algorithm with canonical titration and rGCMCD simulations for different volume fractions of colloidal particles: $\eta = 20\%$ and 30%. Figs. 3 and 4 show that the large deviation of RR-cpH algorithm persists for all studied volume fractions, while rGCMCD and canonical simulation results remain identical.

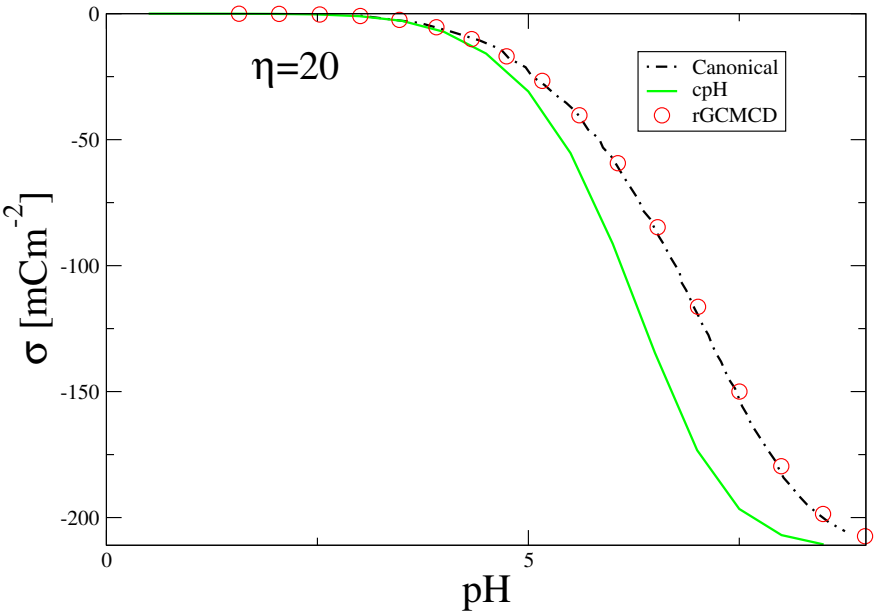

Figure 3: Titration curves obtained using RR-cpH algorithm, canonical titration simulations, and rGCMCD simulation, for colloidal suspension of 20% volume fraction with 10 mM of salt inside the system.

https://doi.org/10.26434/chemrxiv-2024-6tqm6 **ORCID:** https://orcid.org/0000-0001-5448-5179 Content not peer-reviewed by ChemRxiv. **License:** CC BY 4.0

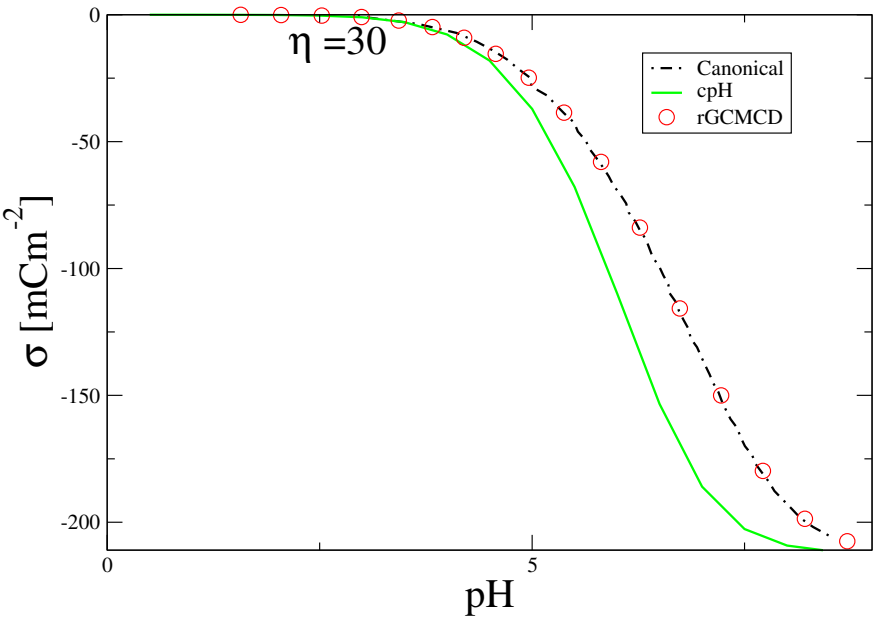

Figure 4: Titration curves obtained using RR-cpH algorithm, canonical titration simulations, and rGCMCD simulation, for colloidal suspension of 30% volume fraction with 10 mM of salt inside the system.

Conclusion

In this paper we have explored the validity of the usual RR-cpH algorithm. Constant pH simulations are now a standard tool for investigating charge regulation in coarse-grained models of proteins, polyelectrolytes, and colloidal systems. It is commonly believed that RR-cpH algorithm can be applied to isolated (canonical) systems. This, however is not the case. The pH specified in the RR-cpH algorithm refers to that of the reservoir, which because of the presence of the Donnan potential can be very different from that of the system. Furthermore, the arbitrary deletions and insertions of ions, which are usually performed to preserve the charge neutrality inside the simulation cell, do not respect the detailed balance condition and can lead to very erroneous results.

To thoroughly investigate this issue, we conducted a comparative analysis of titration curves generated by the standard RR-cpH algorithm and the exact canonical simulation algorithm. The latter incorporates the recently developed surface Widom insertion method

https://doi.org/10.26434/chemrxiv-2024-6tqm6 **ORCID:** https://orcid.org/0000-0001-5448-5179 Content not peer-reviewed by ChemRxiv. **License:** CC BY 4.0

for pH calculation. Our results reveal a substantial disparity between the titration isotherms obtained through the standard RR-cpH algorithm and the canonical titration algorithm. This underscores the critical importance of employing the correct simulation approach when studying charge regulation in polyelectrolytes, proteins, and colloidal systems.

Conflict of Interest

The authors have no conflicts to disclose.

Acknowledgement

This work was partially supported by the CNPq, CAPES, National Institute of Science and Technology Complex Fluids INCT-FCx.

References

(1) Bakhshandeh, A.; Frydel, D.; Levin, Y. Theory of Charge Regulation of Colloidal Particles in Electrolyte Solutions. *Langmuir* **2022**, *38*, 13963–13971.

(2) Frydel, D. General theory of charge regulation within the Poisson-Boltzmann framework: Study of a sticky-charged wall model. *The Journal of Chemical Physics* **2019**, *150*, 194901.

(3) Landsgesell, J.; Nová, L.; Rud, O.; Uhlík, F.; Sean, D.; Hebbeker, P.; Holm, C.; Košovan, P. Simulations of ionization equilibria in weak polyelectrolyte solutions and gels. *Soft Matter* **2019**, *15*, 1155–1185.

(4) Lund, M.; Jönsson, B. On the charge regulation of proteins. *Biochemistry* **2005**, *44*, 5722–5727.

https://doi.org/10.26434/chemrxiv-2024-6tqm6 **ORCID:** https://orcid.org/0000-0001-5448-5179 Content not peer-reviewed by ChemRxiv. **License:** CC BY 4.0

(5) Jiang, T.; Wang, Z.-G.; Wu, J. Electrostatic Regulation of Genome Packaging in Human Hepatitis B Virus. *Biophysical Journal* **2009**, *96*, 3065–3073.

(6) Prusty, D.; Nap, R.; Szleifer, I.; De La Cruz, M. O. Charge regulation mechanism in end-tethered weak polyampholytes. *Soft Matter* **2020**, *16*, 8832–8847.

(7) Lund, M.; Åkesson, T.; Jönsson, B. Enhanced protein adsorption due to charge regulation. *Langmuir* **2005**, *21*, 8385–8388.

(8) Lunkad, R.; Barroso da Silva, F. L.; Košovan, P. Both Charge-Regulation and Charge-Patch Distribution Can Drive Adsorption on the Wrong Side of the Isoelectric Point. *Journal of the American Chemical Society* **2022**, *144*, 1813–1825, PMID: 35048695.

(9) Stornes, M.; Blanco, P. M.; Dias, R. S. Polyelectrolyte-nanoparticle mutual charge regulation and its influence on their complexation. *Colloids and Surfaces A: Physicochemical and Engineering Aspects* **2021**, *628*, 127258.

(10) Curk, T.; Yuan, J.; Luijten, E. Accelerated simulation method for charge regulation effects. *The Journal of Chemical Physics* **2022**, *156*, 044122.

(11) Curk, T.; Luijten, E. Charge Regulation Effects in Nanoparticle Self-Assembly. *Phys. Rev. Lett.* **2021**, *126*, 138003.

(12) Ong, G. M.; Gallegos, A.; Wu, J. Modeling Surface Charge Regulation of Colloidal Particles in Aqueous Solutions. *Langmuir* **2020**, *36*, 11918–11928.

(13) Lunkad, R.; Barroso da Silva, F. L.; Košovan, P. Both Charge-Regulation and Charge-Patch Distribution Can Drive Adsorption on the Wrong Side of the Isoelectric Point. *Journal of the American Chemical Society* **2022**, *144*, 1813–1825.

(14) Avni, Y.; Andelman, D.; Podgornik, R. Charge regulation with fixed and mobile charged macromolecules. *Current Opinion in Electrochemistry* **2019**, *13*, 70–77, Fundamental and Theoretical Electrochemistry Physical and Nanoelectrochemistry.

https://doi.org/10.26434/chemrxiv-2024-6tqm6 **ORCID:** https://orcid.org/0000-0001-5448-5179 Content not peer-reviewed by ChemRxiv. **License:** CC BY 4.0

(15) Podgornik, R. General theory of charge regulation and surface differential capacitance. *The Journal of Chemical Physics* **2018**, *149*, 104701.

(16) Cohen, E. R. *Quantities, units and symbols in physical chemistry*; Royal Society of Chemistry, 2007.

(17) Israelachvili, J. N. *Intermolecular and surface forces*; Academic press, 2011.

(18) Butt, H.-J. A technique for measuring the force between a colloidal particle in water and a bubble. *Journal of Colloid and Interface Science* **1994**, *166*, 109–117.

(19) Levin, Y. Electrostatic correlations: from plasma to biology. *Reports on progress in physics* **2002**, *65*, 1577.

(20) Andelman, D. Introduction to electrostatics in soft and biological matter. *Soft condensed matter physics in molecular and cell biology* **2006**, *6*.

(21) Borkovec, M.; Jönsson, B.; Koper, G. J. M. In *Surface and Colloid Science*; Matijević, E., Ed.; Springer US: Boston, MA, 2001; pp 99–339.

(22) Grahame, D. C. The electrical double layer and the theory of electrocapillarity. *Chemical reviews* **1947**, *41*, 441–501.

(23) Guldbrand, L.; Jönsson, B.; Wennerström, H.; Linse, P. Electrical double layer forces. A Monte Carlo study. *The Journal of chemical physics* **1984**, *80*, 2221–2228.

(24) López-García, J.; Aranda-Rascón, M.; Horno, J. Electrical double layer around a spherical colloid particle: The excluded volume effect. *Journal of Colloid and Interface Science* **2007**, *316*, 196–201.

(25) James, R. O.; Parks, G. A. *Surface and colloid science*; Springer, 1982; pp 119–216.

(26) Attard, P. Recent advances in the electric double layer in colloid science. *Current Opinion in Colloid & Interface Science* **2001**, *6*, 366–371.

https://doi.org/10.26434/chemrxiv-2024-6tqm6 **ORCID:** https://orcid.org/0000-0001-5448-5179 Content not peer-reviewed by ChemRxiv. **License:** CC BY 4.0

(27) Carnie, S. L.; Chan, D. Y.; Gunning, J. S. Electrical double layer interaction between dissimilar spherical colloidal particles and between a sphere and a plate: The linearized poisson-boltzmann theory. *Langmuir* **1994**, *10*, 2993–3009.

(28) Hermansson, M. The DLVO theory in microbial adhesion. *Colloids and surfaces B: Biointerfaces* **1999**, *14*, 105–119.

(29) Ninham, B. W. On progress in forces since the DLVO theory. *Advances in colloid and interface science* **1999**, *83*, 1–17.

(30) Verwey, E. J. W. Theory of the Stability of Lyophobic Colloids. *The Journal of Physical and Colloid Chemistry* **1947**, *51*, 631–636.

(31) Zhou, S. Effective electrostatic interaction between columnar colloids: roles of solvent steric hindrance, polarity, and surface geometric characteristics. *Molecular Physics* **2023**, e2216632.

(32) Zhou, S. Effective electrostatic forces between two neutral surfaces with surface charge separation: Valence asymmetry and dielectric constant heterogeneity. *Molecular Physics* **2022**, *120*, e2094296.

(33) López-Flores, L.; de la Cruz, M. O. Induced phase transformation in ionizable colloidal nanoparticles. *The European Physical Journal E* **2023**, *46*, 1–10.

(34) Zhou, S. Effective electrostatic potential between two oppositely charged cylinder rods in primitive model and extended primitive model electrolytes. *Journal of Statistical Mechanics: Theory and Experiment* **2019**, *2019*, 033213.

(35) Linderstrøm-Lang, K. Om proteinstoffernes ionisation. *Comptes Rendus des Travaux du Laboratorie Carlsberg* **1924**, *15*, 1–29.

https://doi.org/10.26434/chemrxiv-2024-6tqm6 **ORCID:** https://orcid.org/0000-0001-5448-5179 Content not peer-reviewed by ChemRxiv. **License:** CC BY 4.0

(36) Ninham, B. W.; Parsegian, V. A. Electrostatic potential between surfaces bearing ionizable groups in ionic equilibrium with physiologic saline solution. *J. Theor. Biol.* **1971**, *31*, 405–428.

(37) Markovich, T.; Andelman, D.; Podgornik, R. Charge regulation: A generalized boundary condition? *EPL (Europhysics Letters)* **2016**, *113*, 26004.

(38) Bakhshandeh, A.; Frydel, D.; Levin, Y. Charge regulation of colloidal particles in aqueous solutions. *Phys. Chem. Chem. Phys.* **2020**, *22*, 24712–24728.

(39) Bakhshandeh, A.; Frydel, D.; Diehl, A.; Levin, Y. Charge Regulation of Colloidal Particles: Theory and Simulations. *Phys. Rev. Lett.* **2019**, *123*, 208004.

(40) Bakhshandeh, A.; Segala, M.; Escobar Colla, T. Equilibrium Conformations and Surface Charge Regulation of Spherical Polymer Brushes in Stretched Regimes. *Macromolecules* **2022**, *55*, 35–48.

(41) Hosseini, K.; Trus, P.; Frenzel, A.; Werner, C.; Fischer-Friedrich, E. Skin epithelial cells change their mechanics and proliferation upon snail-mediated EMT signalling. *Soft Matter* **2022**, *18*, 2585–2596.

(42) Reed, C. E.; Reed, W. F. Monte Carlo study of titration of linear polyelectrolytes. *The Journal of chemical physics* **1992**, *96*, 1609–1620.

(43) Labbez, C.; Jönsson, B. A new Monte Carlo method for the titration of molecules and minerals. International Workshop on Applied Parallel Computing. 2006; pp 66–72.

(44) Levin, Y.; Bakhshandeh, A. Comment on "Simulations of ionization equilibria in weak polyelectrolyte solutions and gels" by J. Landsgesell, L. Nová, O. Rud, F. Uhlík, D. Sean, P. Hebbeker, C. Holm and P. Košovan, Soft Matter, 2019, 15, 1155–1185. *Soft Matter* **2023**, *19*, 3519–3521.

https://doi.org/10.26434/chemrxiv-2024-6tqm6 **ORCID:** https://orcid.org/0000-0001-5448-5179 Content not peer-reviewed by ChemRxiv. **License:** CC BY 4.0

(45) Levin, Y.; Bakhshandeh, A. A new method for reactive constant pH simulations. *The Journal of Chemical Physics* **2023**, *159*, 111101.

(46) Ullner, M.; Woodward, C. E. Simulations of the titration of linear polyelectrolytes with explicit simple ions: comparisons with screened Coulomb models and experiments. *Macromolecules* **2000**, *33*, 7144–7156.

(47) Košovan, P.; Landsgesell, J.; Nová, L.; Uhlík, F.; Beyer, D.; Blanco, P. M.; Staňo, R.; Holm, C. Reply to the 'Comment on "Simulations of ionization equilibria in weak polyelectrolyte solutions and gels"'by J. Landsgesell, L. Nová, O. Rud, F. Uhlík, D. Sean, P. Hebbeker, C. Holm and P. Košovan, Soft Matter, 2019, 15, 1155–1185. *Soft Matter* **2023**, *19*, 3522–3525.

(48) Smith, W.; Triska, B. The reaction ensemble method for the computer simulation of chemical and phase equilibria. I. Theory and basic examples. *The Journal of chemical physics* **1994**, *100*, 3019–3027.

(49) Johnson, J. K.; Panagiotopoulos, A. Z.; Gubbins, K. E. Reactive canonical Monte Carlo: a new simulation technique for reacting or associating fluids. *Molecular Physics* **1994**, *81*, 717–733.

(50) Bakhshandeh, A.; Levin, Y. Canonical titration simulations. *Phys. Chem. Chem. Phys.* **2023**, *25*, 32800–32806.

(51) Bakhshandeh, A.; Frydel, D.; Levin, Y. Reactive Monte Carlo simulations for charge regulation of colloidal particles. *The Journal of Chemical Physics* **2022**, *156*, 014108.

(52) Bakhshandeh, A.; Levin, Y. Titration in Canonical and Grand-Canonical Ensembles. *The Journal of Physical Chemistry B* **2023**, *127*, 9405–9411, PMID: 37852244.

(53) Landsgesell, J.; Hebbeker, P.; Rud, O.; Lunkad, R.; Košovan, P.; Holm, C. Grand-

https://doi.org/10.26434/chemrxiv-2024-6tqm6 **ORCID:** https://orcid.org/0000-0001-5448-5179 Content not peer-reviewed by ChemRxiv. **License:** CC BY 4.0

reaction method for simulations of ionization equilibria coupled to ion partitioning. *Macromolecules* **2020**, *53*, 3007–3020.

(54) Bakhshandeh, A.; Levin, Y. Widom insertion method in simulations with Ewald summation. *The Journal of Chemical Physics* **2022**, *156*, 134110.

(55) Widom, B. Some topics in the theory of fluids. *The Journal of Chemical Physics* **1963**, *39*, 2808–2812.

(56) Boda, D.; Giri, J.; Henderson, D.; Eisenberg, B.; Gillespie, D. Analyzing the components of the free-energy landscape in a calcium selective ion channel by Widom's particle insertion method. *The Journal of chemical physics* **2011**, *134*, 02B607.

(57) Svensson, B. R.; Woodward, C. E. Widom's method for uniform and non-uniform electrolyte solutions. *Molecular Physics* **1988**, *64*, 247–259.

(58) Sloth, P.; Sørensen, T. S. Monte Carlo calculations of chemical potentials in ionic fluids by application of Widom's formula: Correction for finite-system effects. *Chemical physics letters* **1990**, *173*, 51–56.

(59) de Leeuw, S. W.; Perram, J. W.; Smith, E. R. Simulation of electrostatic systems in periodic boundary conditions. I. Lattice sums and dielectric constants. *Proceedings of the Royal Society of London. A. Mathematical and Physical Sciences* **1980**, *373*, 27–56.

(60) Smith, E. R. Electrostatic energy in ionic crystals. *Proceedings of the Royal Society of London. A. Mathematical and Physical Sciences* **1981**, *375*, 475–505.

(61) Ballenegger, V. Communication: On the origin of the surface term in the Ewald formula. *The Journal of Chemical Physics* **2014**, *140*.

(62) dos Santos, A. P.; Girotto, M.; Levin, Y. Simulations of Coulomb systems with slab geometry using an efficient 3D Ewald summation method. *The Journal of chemical physics* **2016**, *144*.

https://doi.org/10.26434/chemrxiv-2024-6tqm6 **ORCID:** https://orcid.org/0000-0001-5448-5179 Content not peer-reviewed by ChemRxiv. **License:** CC BY 4.0

(63) Euwema, R.; Surratt, G. The absolute positions of calculated energy bands. *Journal of Physics and Chemistry of Solids* **1975**, *36*, 67–71.

https://doi.org/10.26434/chemrxiv-2024-6tqm6 **ORCID:** https://orcid.org/0000-0001-5448-5179 Content not peer-reviewed by ChemRxiv. **License:** CC BY 4.0

Graphical TOC Entry

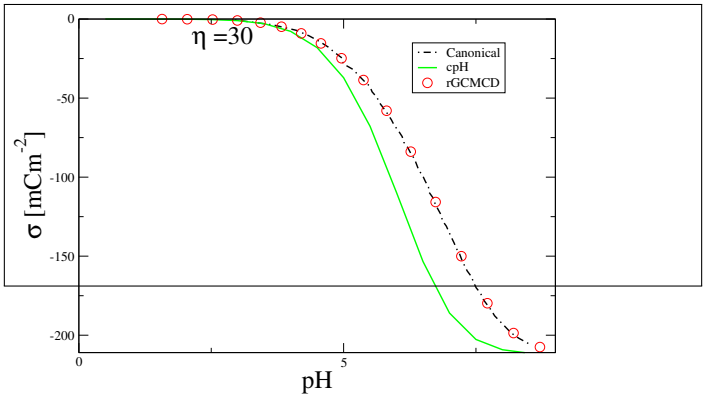

https://doi.org/10.26434/chemrxiv-2024-6tqm6 **ORCID:** https://orcid.org/0000-0001-5448-5179 Content not peer-reviewed by ChemRxiv. **License:** CC BY 4.0